Complex dispersion relation of a double chain of lossy metal nanoparticles

Massimiliano Guasoni, Matteo Conforti

Complex dispersion relation of a double chain of lossy metal nanoparticles

Massimiliano Guasoni and Matteo Conforti

CNISM and Dipartimento di Ingegneria dell'Informazione, Università di Brescia, Via Branze 38, 25123 Brescia, Italy

We study the propagation characteristics of optical signals in waveguides composed of a double chain of metallic nanoparticles embedded in a dielectric host. We find that the complex Bloch band diagram for the guided modes, derived by the Mie scattering theory including material losses, exhibits strong differences with respect to the previously studied single chain. The results of the model are validated through finite element solution of Maxwell's equations.

OCIS codes: 78.67.Bf,42.70.Qs,42.82.Et,71.45.Gm

1. Introduction

Metal optics is becoming a valid route for the miniaturization of photonic circuits [1,2]. Plasmonic waveguides can be realized by exploiting straight metal-dielectic interfaces

[3], slots [4], wedges [5], grooves [6] or linear chains of closely spaced nanoparticles [7–19].

The coupled-dipole approximation (CDA) is usually used in order to calculate the dispersion relation of a linear chain of nanoparticles, where the spheres are treated as point dipoles with a certain polarizability $\alpha(\omega)$. Recently the authors have developed a method to calculate the dispersion relation of a lossy linear chain analytically by means of the Mie theory and numerically by a proper formulation of finite element method for Maxwell Equation [19].

At optical frequency the linear chain is characterized by a trade off between field concentration and propagation losses: the more the field is concentrated around the nanostructure, the more the imaginary part of the mode wavevector is high. A solution to this trade off can be offered by pairing together two chains of nanoparticles [20,21]. This geometry can offer high field confinement between the chains, without giving rise to excessively high propagation losses. This structure has been studied recently by exploiting concepts of optical nanocircuits, and two propagating modes have been identified [21].

In this paper we derive the dispersion relation of the first six modes for couples of nanoparticle chains by exploiting Mie scattering method.

We calculate the complex band diagram by numerically solving the dispersion relation for lossy particles, by fixing a real frequency and finding a complex wavevector. We find a complex dispersion relation where the real part of the propagation constant

is modified by the losses.

To conclude we compare the results of the Mie model with the exact Bloch modes dispersion calculated by means of a revised finite element method formulation of Maxwell's equations in which, as explained in [19], frequency is a parameter and the strong dispersion of the metal is easily taken into account.

The paper is organized as follows. In Sec. II and III we find the complex dispersion relation of a double chain of nanoparticles following the Mie scattering approach. We show that, differently from the case of a **uniform** single chain **(see [19])**, the dispersion relations cannot be expressed as a linear combination of polylogarithms but they need to be calculated as a linear combination of Lerch functions. The treatment can also be applied to calculate the dispersion relations of a non-uniform single chain, in which the center-to-center distances between spheres are not constant but are alternated.

In Sec. IV we analyze the dispersion relation in a case of interest, that is two parallel chains of nanoparticles. We put in evidence that six non degenerate modes exist differently from the case of the single chain, where only two non degenerate modes exist **(see [19])**. We also highlight that in four of this six modes there is a coupling interaction between the transverse mode of a chain and the longitudinal mode of the other chain (and viceversa). In the end we also show that the useful transmission band of the double chain can be much greater than the band of the single chain (until five times, **see [19]**). In Sec. V we compare the results of the

finite element simulation with those of the analytical approach. Sec. VI contains the concluding remarks.

The use of Lerch functions, the possibility of treating the non uniform single chain, the demonstration of the existence of six modes and the increased useful band are the main achievements of this work with respect to the previous regarding the uniform single chain (such as in [19]).

2. Dispersion relation of a double chain of nanoparticles: Mie theory approach

In this section we exploit the generalized Mie theory of Gerardy-Ausloos [22] to study the properties of a double chain of nanospheres. The nanospheres in both chains have radius R, center-to-center spacing d, dielectric constant ϵ_s, and are embedded in an infinite matrix with dielectric constant ϵ_m. The two chains, that we assume, without loss of generality, to be disposed on the $x-y$ plane, are aligned along the x axis, are separated by a distance L on the y axis and a displacement s on the x axis (see Fig.1).

As explained in [22], the total electric field is a linear combination of the vector spherical harmonics (VSH) of the first and third kind $\overrightarrow{m}^1_{lm}(n)$, $\overrightarrow{n}^1_{lm}(n)$, $\overrightarrow{m}^3_{lm}(n)$ and $\overrightarrow{n}^3_{lm}(n)$ centered in the $n-$th sphere, where l sweeps from 1 to infinity, while m from $-l$ to $+l$. The VSH of the third kind are generated by the scattering of the VSH of the first kind, and are linked to each other by means of the scattering coefficients Γ_l and

Δ_l. When the radius R is sufficiently smaller than the wavelength of the input field only the coefficient Δ_1 is significant, so that a great simplification of the treatment occurs because only the vector functions $\overrightarrow{n}^1_{1-1}$, $\overrightarrow{n}^1_{10}$, $\overrightarrow{n}^1_{11}$, $\overrightarrow{n}^3_{1-1}$, $\overrightarrow{n}^3_{10}$ and $\overrightarrow{n}^3_{11}$ need to be considered (see [19]). By following the treatment described in [19], it is then possible to write for the $n-$th sphere:

$$b_{i,1m}(n) = \Delta_1^{-1} d_{1m}(n) - \sum_{v \neq n} \sum_{q=-1}^{1} T_{1q1m}(v,n) d_{1q}(v) \tag{1}$$

where $m = \{-1, 0, 1\}$ and $b_{i,1m}(n)$ are the coefficients of the linear combination related to the vector functions $\overrightarrow{n}^1_{1m}(n)$ that represent the incident field, while $d_{1m}(n)$ are the coefficients related to $\overrightarrow{n}^3_{1m}(n)$ that represent the scattered field. $T_{1q1m}(v,n)$ is the coupling coefficient between $\overrightarrow{n}^1_{1m}(n)$ and $\overrightarrow{n}^3_{1q}(v)$ in the n-th frame. Once the incident field is known (i.e. the coefficients $b_{i,1m}(n)$ for any sphere), the scattered field can be calculated by solving the system (1) for the coefficients $d_{1m}(n)$. The coupling coefficients can be easily calculated by means of simple analytical formulas [23] and when the spheres are located on the $x-y$ plane, we have $T_{101-1}(v,n) = T_{1011}(v,n) = T_{1-110}(v,n) = T_{1110}(v,n) = 0$, so that the functions $\overrightarrow{n}^1_{10}$ (respectively $\overrightarrow{n}^3_{10}$) are decoupled from $\overrightarrow{n}^3_{1-1}$ and $\overrightarrow{n}^3_{11}$ (respectively $\overrightarrow{n}^1_{1-1}$ and $\overrightarrow{n}^1_{11}$). Let's now distinguish the even spheres, that are in the right chain, from the odd spheres, that are in the left chain (see Fig.1). Then it is possible to write, for the coefficients d_{10}:

$$b_{i,10}(2n) = \Delta_1^{-1} d_{10}(2n) - \sum_{v \neq n} T_{1010}(2v, 2n) d_{10}(2v) - \\ - \sum_{v} T_{1010}(2v+1, 2n) d_{10}(2v+1), \tag{2}$$

$$b_{i,10}(2n+1) = \Delta_1^{-1} d_{10}(2n+1) - \\ - \sum_{v} T_{1010}(2v, 2n+1) d_{10}(2v) - \\ - \sum_{v \neq n} T_{1010}(2v+1, 2n+1) d_{10}(2v+1). \tag{3}$$

Let's now denote with E and O the quantities related to the even and the odd spheres, respectively. We adopt the notation: $b_{i,10}(2n) = b_{i,10E}(n)$, $b_{i,10}(2n+1) = b_{i,10O}(n)$, $d_{10}(2n) = d_{10E}(n)$, $d_{10}(2n+1) = d_{10O}(n)$, $-T_{1010}(2v, 2n) = -T_{1010}(2v+1, 2n+1) = U_{1010}(v, n)$, $-T_{1010}(2v+1, 2n) = E_{1010}(v, n)$, $-T_{1010}(2v, 2n+1) = O_{1010}(v, n)$. Being the spacing d constant in the two chains $U_{1010}(v, n) = U_{1010}(v-n)$ and similarly for the other coupling coefficients (v, n) can be substituted by $(v-n)$, so that the equations Eq.(2) and Eq.(3) are conveniently rewritten as:

$$b_{i,10E}(n) = \Delta_1^{-1} d_{10E}(n) + \sum_{v \neq n} U_{1010}(v-n) d_{10E}(v) + \\ + \sum_{v} E_{1010}(v-n) d_{10O}(v), \tag{4}$$

$$b_{i,10O}(n) = \Delta_1^{-1} d_{10O}(n) + \sum_v O_{1010}(v-n) d_{10E}(v) + \\ + \sum_{v \neq n} U_{1010}(v-n) d_{10O}(v). \quad (5)$$

By defining $U_{1010}(0) = \Delta_1^{-1}$ it is possible to rewrite Eq.(4) and Eq.(5) by means of the convolution operator $*$:

$$b_{i,10E}(n) = U_{1010}(n) * d_{10E}(n) + E_{1010}(n) * d_{10O}(n), \quad (6)$$

$$b_{i,10O}(n) = O_{1010}(n) * d_{10E}(n) + U_{1010}(n) * d_{10O}(n). \quad (7)$$

Finally, the equations (6-7) can be rewritten in the spatial frequency domain by using the Discrete Time Fourier Transform (DTFT):

$$M_A \begin{bmatrix} \hat{d}_{10E}(k) \\ \\ \hat{d}_{10O}(k) \end{bmatrix} = \begin{bmatrix} \hat{b}_{i,10E}(k) \\ \\ \hat{b}_{i,10O}(k) \end{bmatrix} \quad (8)$$

where

$$M_A = \begin{bmatrix} \hat{U}_{1010}(k) & \hat{E}_{1010}(k) \\ \\ \hat{O}_{1010}(k) & \hat{U}_{1010}(k) \end{bmatrix}. \quad (9)$$

where the accent $\hat{}$ denotes the DTFT.

All the treatment can be repeated for the coefficients $b_{i,1-1}$, $b_{i,11}$, d_{1-1} and d_{11}: let's call $b_{i,1m}(2n) = b_{i,1mE}(n)$, $b_{i,1m}(2n+1) = b_{i,1mO}(n)$, $d_{1m}(2n) = d_{1mE}(n)$, $d_{1m}(2n+1) =$

$d_{1mO}(n)$, $-T_{1l1m}(2v,2n) = -T_{1l1m}(2v+1,2n+1) = U_{1l1m}(v-n)$, $-T_{1l1m}(2v+1,2n) = E_{1l1m}(v-n)$, $-T_{1l1m}(2v,2n+1) = O_{1l1m}(v,n)$, with l and $m = -1, 1$, then considering that $U_{1-11-1}(0) = U_{1111}(0) = \Delta_1^{-1}$ and $U_{1-111}(0) = U_{111-1}(0) = 0$ and using the DTFT we can write:

$$M_B \begin{bmatrix} \hat{d}_{11E}(k) \\ \hat{d}_{1-1E}(k) \\ \hat{d}_{11O}(k) \\ \hat{d}_{1-1O}(k) \end{bmatrix} = \begin{bmatrix} \hat{b}_{i,11E}(k) \\ \hat{b}_{i,1-1E}(k) \\ \hat{b}_{i,11O}(k) \\ \hat{b}_{i,1-1O}(k) \end{bmatrix} \tag{10}$$

where

$$M_B = \begin{bmatrix} \hat{U}_{1111}(k) & \hat{U}_{1-111}(k) & \hat{E}_{1111}(k) & \hat{E}_{1-111}(k) \\ \hat{U}_{111-1}(k) & \hat{U}_{1-11-1}(k) & \hat{E}_{111-1}(k) & \hat{E}_{1-11-1}(k) \\ \hat{O}_{1111}(k) & \hat{O}_{1-111}(k) & \hat{U}_{1111}(k) & \hat{U}_{1-111}(k) \\ \hat{O}_{111-1}(k) & \hat{O}_{1-11-1}(k) & \hat{U}_{111-1}(k) & \hat{U}_{1-11-1}(k) \end{bmatrix} \tag{11}$$

Following the treatment in [23] it is possible to find analytical formulas for the coupling coefficients:

$$
\begin{aligned}
U_{1010}(n) &= i\frac{3}{2}\frac{e^{id_U(n)}}{d_U(n)} - \frac{3}{2}\frac{e^{id_U(n)}}{d_U(n)^2} - i\frac{3}{2}\frac{e^{id_U(n)}}{d_U(n)^3},\ n \neq 0 \\
U_{1111}(n) &= i\frac{3}{4}\frac{e^{id_U(n)}}{d_U(n)} + \frac{3}{4}\frac{e^{id_U(n)}}{d_U(n)^2} + i\frac{3}{4}\frac{e^{id_U(n)}}{d_U(n)^3},\ n \neq 0 \\
U_{1-111}(n) &= -i\frac{3}{4}\frac{e^{id_U(n)}}{d_U(n)} + \frac{9}{4}\frac{e^{id_U(n)}}{d_U(n)^2} + i\frac{9}{4}\frac{e^{id_U(n)}}{d_U(n)^3},\ n \neq 0 \\
E_{1010}(n) &= i\frac{3}{2}\frac{e^{id_E(n)}}{d_E(n)} - \frac{3}{2}\frac{e^{id_E(n)}}{d_E(n)^2} - i\frac{3}{2}\frac{e^{id_E(n)}}{d_E(n)^3}, \\
E_{1111}(n) &= i\frac{3}{4}\frac{e^{id_E(n)}}{d_E(n)} + \frac{3}{4}\frac{e^{id_E(n)}}{d_E(n)^2} + i\frac{3}{4}\frac{e^{id_E(n)}}{d_E(n)^3}, \\
E_{1-111}(n) &= -i\frac{3}{4}\frac{e^{id'_E(n)}}{d_E(n)} + \frac{9}{4}\frac{e^{id'_E(n)}}{d_E(n)^2} + i\frac{9}{4}\frac{e^{id'_E(n)}}{d_E(n)^3}, \\
E_{111-1}(n) &= -i\frac{3}{4}\frac{e^{id''_E(n)}}{d_E(n)} + \frac{9}{4}\frac{e^{id''_E(n)}}{d_E(n)^2} + i\frac{9}{4}\frac{e^{id''_E(n)}}{d_E(n)^3},
\end{aligned}
\tag{12}
$$

where $d_U(n)$ is the distance between the $2m$ sphere and the $2(m+n)$ sphere in the right chain (or equivalently between the $2m+1$ sphere and the $2(m+n)+1$ sphere in the left chain) normalized respect to the wave-vector k_M in the matrix (that is $d_U(n) = k_M d|n|$). Similarly $d_E(n)$ indicates the normalized distance between the $2m$ sphere in the right chain and the $2(m+n)+1$ sphere in the left chain, that is $d_E(n) = k_M\sqrt{L^2 + (dn+s)^2}$. Besides $d'_E(n) = d_E(n) - 2\beta(n)$, where $\beta(n)$ is the angle between these two last spheres (see Fig.1), and $d''_E(n) = d_E(n) + 2\beta(n)$. Moreover, the subsequent equalities hold true: $U_{111-1}(n) = U_{1-111}(n)$, $U_{1111}(n) = U_{1-11-1}(n)$, $E_{1111}(n) = E_{1-11-1}(n)$, $O_{1111}(n) = O_{1-11-1}(n)$ and $O_{1l1m}(n) = E_{1l1m}(-n)$ (l and $m = \{-1, 1\}$).

As consequence, in the matrix M_B (11) $\hat{U}_{111-1}(k) = \hat{U}_{1-111}(k)$, $\hat{U}_{1111}(k) = \hat{U}_{1-11-1}(k)$, $\hat{E}_{1111}(k) = \hat{E}_{1-11-1}(k)$, $\hat{O}_{1111}(k) = \hat{O}_{1-11-1}(k)$ and $\hat{O}_{1l1m}(k) = \hat{E}_{1l1m}(-k)$ (l and

$m = \{-1, 1\}$).

In order to find the propagating modes of the double chain we proceed as follows: we fix a value of frequency ω and impose a vanishing input field (i.e. $b_{i,1-1}(n) = b_{i,10}(n) = b_{i,11}(n) = 0$). We then search for values of wavevector k that give nontrivial solutions of systems (9) and (10), by imposing $Det(M_A(k)) = 0$ and $Det(M_B(k)) = 0$. These values of k represent the propagation constants of the modes normalized respect to the period d of the system. The corresponding coefficients $d_{lmE}(n)$ and $d_{lmO}(n)$ (l and $m = \{-1, 0, 1\}$) are of the form $D(k)e^{ikn}$ ($D(k)$ constant independent on n). In the next section we discuss about the search of k in the complex plane.

3. Derivation of the complex dispersion relations

Being the system periodic, the real part of k falls between 0 and π. It is possible to show that under the condition of k real and $k_M d < k < \pi$ (i.e. under the light line) the DTFTs in M_A and M_B except $\hat{U}_{1010}(k)$ and $\hat{U}_{1111}(k)$ have a vanishing real part, and $\mathrm{Re}(\hat{U}_{1010}(k) - \Delta_1^{-1})= \mathrm{Re}(\hat{U}_{1111}(k) - \Delta_1^{-1})=1$. If the system is lossless it is also verified that $\mathrm{Re}(\Delta_1^{-1})$=-1 [19], implying $\mathrm{Re}(\hat{U}_{1010}(k))= \mathrm{Re}(\hat{U}_{1111}(k))=0$. To sum up, in a lossless system the DTFTs in M_A and M_B have vanishing real part if $k_M d < k < \pi$, making $Im[Det(M_A(k))] = Im[Det(M_B(k))] = 0$; then it is possible to find modes that propagates without damping by looking for real k between $k_M d$ and π that solve $Re[Det(M_A(k))] = 0$ or $Re[Det(M_B(k))] = 0$. It is worth noting that, being k real, these last two equations are well-posed because the summations in

the DTFTs converge and can be evaluated by truncating them to a finite number of terms.

When the system is lossy $Re(\Delta_1^{-1}) \neq -1$, then $Re(\hat{U}_{1010}(k)) \neq 0$ and $\mathrm{Re}(\hat{U}_{1111}(k)) \neq 0$. In this case $Im[Det(M_A(k))] \neq 0$ and $Im[Det(M_B(k))] \neq 0$ even for k under the light line. As a consequence $Det(M_A(k)) = 0$ and $Det(M_B(k)) = 0$ have no real solutions, and solutions have to be found in the complex plane. This means that the modes propagate necessary with damping. In this case, being k complex, the DTFTs of $M_A(k)$ and $M_B(k)$ diverge, making the problem ill-posed.

In [19] it is shown that $\hat{U}_{1l1m}(k)$ (for l and $m = \{-1, 0, 1\}$) can be rewritten as sum of polylogarithms and then evaluated by exploiting analytic continuation as suggested by Citrin [14], so that the difficulties entailed by the presence of a complex k can be overcome. The other DTFTs can not be expressed directly as sum of polylogarithms because of the term $\sqrt{L^2 + (dn + s)^2}$ in $d_E(n)$. However we can manage to write them as functions that admit an analytic continuation, in order to avoid the divergence problem. Let's then take first of all the case of $L = 0$, so that $d_E(n) = k_M|dn + s|$ and let's consider, as example, the DTFT $\hat{E}_{1010}(k)$:

$$\hat{E}_{1010}(k) = E_{1010}(0) + \\ + \sum_{v=1}^{3} a_v \left[\sum_{n=1}^{\infty} \frac{e^{ik_M(dn+s)-ikn}}{k_M^v(dn+s)^v} + \sum_{n=1}^{\infty} \frac{e^{ik_M(dn-s)+ikn}}{k_M^v(dn-s)^v} \right] \tag{13}$$

where $a_1 = (3i/2)$, $a_2 = -(3/2)$ and $a_3 = -(3i/2)$. The summations in n can be

expressed by means of Lerch functions [24] that, similarly to polylogarithms, admit analytic continuation. In fact the following relation holds true:

$$\sum_{n=1}^{\infty} \frac{e^{ik_M(dn\mp s)\pm ikn}}{k_M^v (dn \mp s)^v} = (k_M d)^{-v} e^{ik_M(d\mp s)\pm ik} Lerch(e^{ik_M d \pm ik}, v, 1 \mp (s/d)) \tag{14}$$

Then $\hat{E}_{1010}(k)$ can be written as linear combination of Lerch functions, and similarly all the other DTFTs in $M_A(k)$ and $M_B(k)$, so that analytic continuation is possible for all them.

In this way the divergence problem in the evaluation of $Det(M_A(k))$ and $Det(M_B(k))$ is avoided, and complex solutions k can be found in the case $L = 0$. This case corresponds to a non uniform linear chain of spheres whose center-to-center distance is not constant but is, alternately, s and $(d - s)$.

When $L \neq 0$ it is not possible to write the DTFTs as combination of Lerch functions. In this case we expand them in a Taylor series in L around $L = 0$. In particular, let's consider the infinite summations in n of the DTFTs, that posses the form $\sum_{n=1}^{\infty} f(n)$, with $f(n) = e^{ik_M\sqrt{L^2+(dn\mp s)^2}\pm ikn}/[k_M^v \sqrt{L^2 + (dn \mp s)^2}]^v$ $(v = 1, 2, 3)$. We note that any term $f(n)$ can be expanded in Taylor series $f_T(n)$ about 0 only if $|L| < |(dn \mp s)|$. Let's then take the first N for which $|L| < |(dN \mp s)|$ and rewrite the sums in the following way:

$$\sum_{n=1}^{\infty} f(n) = \sum_{n=1}^{N-1} f(n) + \sum_{n=N}^{\infty} f(n) \approx \sum_{n=1}^{N-1} f(n) + \sum_{n=N}^{\infty} f_T(n) = \\ = \sum_{n=1}^{\infty} f_T(n) + \sum_{n=1}^{N-1} (f(n) - f_T(n)) \tag{15}$$

where the approximation $f_T(n) \approx f(n)$ is done for $n \geq N$. The term $\sum_{n=1}^{N-1}(f(n) - f_T(n))$ does not diverge because it is made over a finite number of elements and the term $\sum_{n=1}^{\infty} f_T(n)$ can be expressed as a linear combination of Lerch functions. To summarize, we succeeded in approximating any infinite summation in the DTFTs as a sum between a linear combination of Lerch functions ($\sum_{n=1}^{\infty} f_T(n)$) and the finite term $\sum_{n=1}^{N-1}(f(n) - f_T(n))$: in this way we can exploit analytic continuation. Let's note that the approximations can be improved at will by considering a sufficiently high number of terms in the Taylor expansion.

Let us note that the proposed methodology can be extended by taking into account for higher order VHS (but at the price of a major complexity) so that spheres whose radius is not much smaller than the wavelength could be taken into account.

Note also that the developed approach is valid for strictly spherical particles, but a modified version of Mie theory exists for ellipsoidal particles, and our methodology can in principle be applied exploiting this theory. The derivation of our method for chains with ellipsoidal particles follows strictly the method described for chains with spherical particles.

We conclude by noting that the derived theory can represent also the core of the method to find the modes of other guiding structures, such as plasmonic photonic crystal waveguides or arrays.

4. Design and analysis of a double-chain without displacement

In this section we calculate the dispersion curves for a case of interest by considering two parallel chains of silver spheres embedded in glass ($\epsilon_m = 2.25$) with null displacement $s = 0$, period $d = 75nm$, distance between the chains $L = 75nm$, radius $R = 25nm$. The dielectric constant $\epsilon_s(\omega)$ of the spheres is calculated by means of a fitting model based on values tabulated by Johnson and Christy in [25]. We decided to avoid the popular Drude model because it is not accurate in the visible range, expecially for what concern absorption.

It is well known (see for example [19], [14] or [10]) that the single chain has two transverse (T_1 and T_2) and one longitudinal (L) modes. The two transverse modes are degenerate because the second is simply a ninety-degree rotation of the first around the axis of the chain.

The modes T_1 and T_2 are found by solving $\hat{U}_{1010}(k) = 0$ and the corresponding electric fields can be written respectively as $\sum_n \overrightarrow{n}^3_{10}(n)e^{ikn}$ and $\sum_n(\overrightarrow{n}^3_{11}(n) - \overrightarrow{n}^3_{1-1}(n))e^{ikn}$; whereas L is found by solving $\hat{U}_{1111}(k)+\hat{U}_{111-1}(k) = 0$ and the corresponding electric field is $\sum_n(\overrightarrow{n}^3_{11}(n) + \overrightarrow{n}^3_{1-1}(n))e^{ikn}$.

In the double chain, since the functions $\overrightarrow{n}^1_{10}$ are decoupled from $\overrightarrow{n}^3_{1-1}$ and $\overrightarrow{n}^3_{11}$, the

mode T_1 of the left (rigth) chain is decoupled from the modes T_2 and L of the right (left) chain. In this way we find that two modes of the double chain are generated by the coupling of the modes T_1 of the isolated chains. These modes are found by solving $Det(M_A(k)) = 0$. Having assumed $s = 0$ we have that $\hat{E}_{1010}(k) = \hat{O}_{1010}(k)$, so that $Det(M_A(k)) = 0$ implies $\hat{U}_{1010}(k) \pm \hat{E}_{1010}(k) = 0$, and $d_{10E}(n) = \pm d_{10O}(n)$. Then the solution of $\hat{U}_{1010}(k) + \hat{E}_{1010}(k) = 0$ corresponds to a transverse mode T_{1i} in which the two T_1 modes of the single chains propagate in phase; whereas the solution of $\hat{U}_{1010}(k) - \hat{E}_{1010}(k) = 0$ correspond to a transverse mode T_{1a} in which the two T_1 modes of the single chains propagate in antiphase.

The mode T_2 of the single left (rigth) chain is not decoupled from the mode L of the right (left) chain, and vice versa, so we expect that in the double chain some modes exist that are combinations of T_2 and L. They can be found by solving $Det(M_B(k)) = 0$. Let's note that, being $s = 0$, $\hat{E}_{1111}(k) = \hat{O}_{1111}(k)$, $\hat{E}_{1-111}(k) = \hat{O}_{111-1}(k)$ and $\hat{E}_{111-1}(k) = \hat{O}_{1-111}(k)$. It is easy to prove that in this case the matrix $M_B(k)$ has eigenvectors $[\hat{d}_{11E}(k), \hat{d}_{1-1E}(k), \hat{d}_{11O}(k), \hat{d}_{1-1O}(k)]$ of the form $[a, b, b, a]$ or $[a, b, -b, -a]$. In the first case we can write

$$[a, b, b, a] = (a/2 + b/2)[1, 1, 1, 1] + (a/2 - b/2)[1, -1, -1, 1]$$

that means that the electric field given by the left chain is

$$\sum_n \frac{a+b}{2}[\overrightarrow{n}^3_{11}(n) + \overrightarrow{n}^3_{1-1}(n)]e^{ikn} +$$
$$+\sum_n \frac{a-b}{2}[\overrightarrow{n}^3_{11}(n) - \overrightarrow{n}^3_{1-1}(n)]e^{ikn}$$

while the electric field given by the right chain is

$$\sum_n \frac{a+b}{2}[\overrightarrow{n}^3_{11}(n) + \overrightarrow{n}^3_{1-1}(n)]e^{ikn} -$$
$$-\sum_n \frac{a-b}{2}[\overrightarrow{n}^3_{11}(n) - \overrightarrow{n}^3_{1-1}(n)]e^{ikn}$$

Then in the left chain the linear combination of L and T_2 is $(a/2+b/2)L+(a/2-b/2)T_2$, while in the right chain is $(a/2+b/2)L-(a/2-b/2)T_2$ (modes L in phase, T_2 in antiphase).

Similar arguments hold true when the eigenvector is of the form $[a, b, -b, -a]$: in this case in the left chain the linear combination of L and T_2 is $-(a/2+b/2)L+(a/2-b/2)T_2$, while in the right chain is $(a/2+b/2)L+(a/2-b/2)T_2$ (modes L in antiphase, T_2 in phase). The coefficients $(a/2+b/2)$ and $(a/2-b/2)$ give more or less weight to the modes L and T_2 in the linear combination. We expect that, if for a fixed frequency ω only the mode T_2 propagates in the single chain ($1.3 < \omega d < 1.65$ in Fig.3), then in the double chain it is dominant with respect to L ($(a/2+b/2) << (a/2-b/2)$), so we can define two modes where T_2 is dominant over L, in which T_2 is in phase and L in anti-phase ($T_{2i}L_a$) or vice versa ($T_{2a}L_i$), on the basis of what we stated above. Conversely, if for a fixed pulsation ω only the mode L propagates in the single chain

($\omega d > 1.65$ in Fig.5), then L is dominant over T_2 in the double chain, so we can define two modes ($L_i T_{2a}$) and ($L_a T_{2i}$) in which the two L modes of the single chains are in phase or antiphase respectively (and vice versa for the T_2 modes).

In Fig.2, Fig.3, Fig.4 and Fig.5 we plot the dispersion curves ($Re(k)$) and the losses of the modes ($Im(k)$) in the single chain and in the double chain. Being the system lossy, in order to calculate the DTFTs of $M_A(k)$ and $M_B(k)$, we exploited the procedure described in the previous section, using Eq.(15), stopping the correspondent Taylor series at the eighth order. Moreover we analyzed the eigenvectors of $M_B(k)$ (the coefficients $(a/2 \pm b/2)$) in order to understand if the components T_2 and L are in phase or in antiphase, and if T_2 is dominant over L or vice versa.

We note that at low frequencies ($\omega d < 1.65$) we have the modes T_{1i} and $T_{2i} L_a$ (T_2 is dominant), because in this range only T_1 andT_2 are allowed in the single chain. Indeed the dispersion curve of $T_{2a} L_i$ lies in between those of T_2 and L of the single chain, because it's in the range of frequencies ($1.56 < \omega d < 1.72$) in which them both exist in the single chain, so they have nearly the same weight in the linear combination that generates $T_{2a} L_i$; the curve of $T_{2a} L_i$ flows into that of $L_i T_{2a}$ for frequencies $\omega d > 1.72$, for which L start to be dominant over T_2.

We can also observe that losses are acceptable only for modes $T_{2i} L_a$ and T_{1i} and at low frequencies; this is due to the fact that for the other modes and at high frequencies the electric field is almost concentrated around the metal spheres, increasing in this way the absorption.

Let's conclude by noting that in the double chain the useful transmission band is greater than in the single chain. If we require a decay length of $5\mu m$ and a transverse mode decay at $1/e$ of $50nm$, the sum of the useful bands of modes T_{1i} ($1.34 < \omega d < 1.45$) and $T_{2i}L_a$ ($1.24 < \omega d < 1.34$) in the double chain is nearly five times greater than the useful band of T_1 in the single chain ($1.44 < \omega d < 1.48$).

5. Finite element simulations

We calculated the dispersion curves ($Re(k)$) and the losses ($Im(k)$) of the modes in the double chain by solving Maxwell's equations with a finite element method, in order to asses the validity of the theoretical results. When calculating the Bloch modes it is usual to fix the wavevector and to find the frequency by solving a linear eigenvalue problem: in our case, being the metal dispersive, this requires an iterative cycle. Moreover the wavevectors are complex due to material losses, making the iterative search even harder. In order to avoid these difficulties, we used a different approach reformulating the problem into a quadratic eigenvalue problem where the frequency is fixed and the wavevector is searched. The description of this formulation is reported in [19].

As it can be seen in Fig.3, Fig.4 and Fig.5 the curves of modes T_{1i}, T_{1a} and $T_{2i}L_a$ calculated with the FEM match quite perfectly those predicted both in the real and the imaginary part. As far as the other modes are concerned, we can notice that FEM results are greater of nearly the 10% for the real part; even greater errors are

present in the imaginary part. This is due to the fact that the curves of these modes stay in a range of high frequencies, for which the influence of high order VSH is not neglectable, so that our model can not describe accurately the dipersion relations. Let's note that, as predicted, losses are acceptable only at low frequencies for modes $T_{2i}L_a$ and T_{1i}, making them usefull for transmission, and also note that all the modes have a band folding for which it is impossible to reach a zero group velocity [19].

Fig. 6 shows the magnetic field of mode T_1 in the single chain and of modes T_{1i} and T_{1a} in the double chain over the $y-z$ plane: only the component H_x is shown because H_y and H_z are vanishing over this plane. It is clear that T_{1i} is the sum of the two T_1 modes of the single chains that propagate in phase, as expected, while T_{1a} is sum of the two T_1 modes that propagates in antiphase.

In Fig.7 the magnetic field of modes T_2 and L in the single chain and of modes $T_{2i}L_a$, $T_{2a}L_i$ and L_iT_{2a} in the double chain is shown over the $yz-$ plane. As it was stated in the previous section, the mode $T_{2i}L_a$ is the combination of the two T_2 modes of the single chains in phase and of the two L modes in antiphase, and the most of the energy is carried by the T_2 modes. Fig.7 c) fully confirms this scenario: the components H_y and H_z, that are absent in the mode T_2 of the single chain, are due to the presence of the L modes, but they are negligible respect to H_x, that is the only non vanishing component of T_2.

Indeed Fig.7 e) shows that the situation is reversed respect to Fig.7 c): for the mode L_iT_{2a} the main modes in combination are the two L modes in phase, so that com-

ponents H_y and H_z are much greater than H_x, that is absent in the mode L of the single chain and in this case is due to the presence of the T_2 modes. In Fig.7 d) the mode $T_{2a}L_i$ is shown: as observed in the previous section, in this case the modes L and T_2 have nearly the same weight in the combination, that is confirmed from the fact that H_x is comparable with H_y and H_z.

On the basis of the obtained results it is clear that the main limitation of the proposed theoretical model to a full numerical solution is that it is accurate when the particles are sufficiently small with respect to wavelength, in order to excite only first order spherical harmonic. If this condition is not fulfilled some errors are present (of the order of 10% **in our simulations). Nevertheless we highlight that in cases of applicative interest the useful modes stay in the band in which the above condition is respected and that the proposed methodology is order of magnitude faster and requires a negligible memory consumption respect to a numerical solution.**

6. Conclusions

In this paper we derived the complex dispersion relation of a double chain of lossy spheres by using the Mie theory and considering the interaction between spherical vector harmonics of the first order, that is a very good approximation when the radius R of the spheres is sufficiently smaller then the wavelength.

The search of the roots of the dispersion relations requires the evaluation of some

DTFTs for which divergence problems arise due to the complex nature of the solution k. In order to avoid these problems the DTFTs have been approximated by means of Lerch functions for which analytic continuation is possible. Moreover, the pursued analysis gives the exact solution for the case of two chains with vanishing distance L, that corresponds to a single non uniform binary chain.

As an example, a practical case of two parallel chains without displacement has been analyzed: six modes are present, that correspond to the coupling interaction between the transverse and longitudinal modes of the single chains. We have shown that in this interaction the weight of the transverse component can be very different respect to the weight of the longitudinal one and that only two modes have a degree of losses that allows for a propagation over a reasonably long distance. The main goal achieved is that the total useful band is nearly 5 times that of the single chain.

To conclude, all the results has been compared with finite element solutions of the Maxwell's equations.

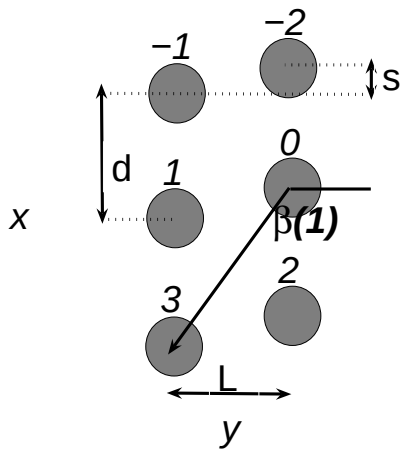

Fig. 1. The system analyzed in this paper consists of two chains of spheres over the xy plane. The chains have distance L, displacement s along the x axis and the spheres (of radius R) in the chains have center-to-center distance d. Odd spheres stay in the left chain, even spheres in the right chain. Note as example the angle $\beta(1)$ between the spheres 0 and 3.

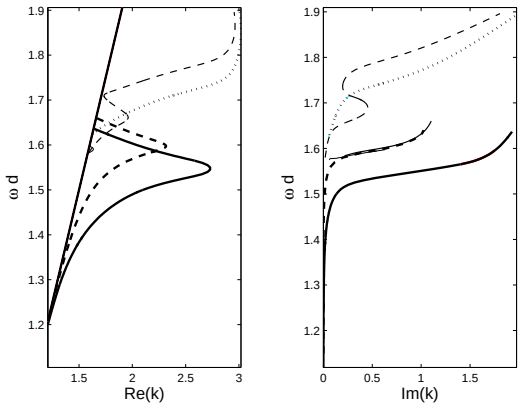

Fig. 2. General view of the real and imaginary part of $k(\omega)$ for the theoretically predicted modes in the double chain. Black dashed and bold line is mode T_{1i}; black bold line is $T_{2i}L_a$; black thin line is T_{1a}; black dashed and thin line is $T_{2a}L_i$ together with L_iT_{2a}; black dotted line is L_aT_{2i}. Real part represent the dispersion curve of the mode, imaginary part its losses.

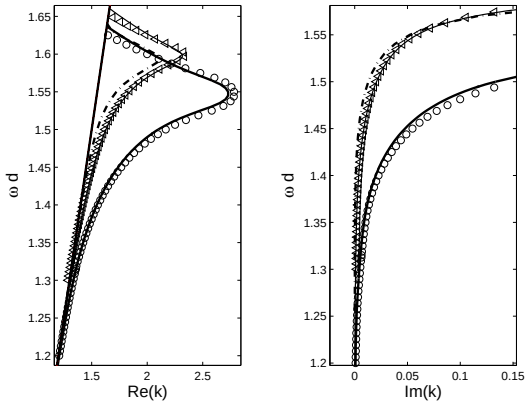

Fig. 3. Real and imaginary part of $k(\omega)$ for the mode T_{1i} (theoretical results: black thin line; FEM results: triangles) and $T_{2i}L_a$ (theoretical results: black bold line; FEM results: circles). The black dashdot line is relative to mode T_1 and T_2 in the single chain.

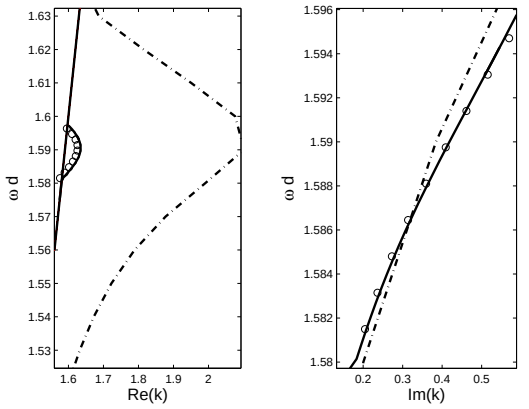

Fig. 4. Real and imaginary part of $k(\omega)$ for the mode T_{1a} (theoretical results: black bold line; FEM results: circles). The black dashdot line is relative to mode T_1 and T_2 in the single chain.

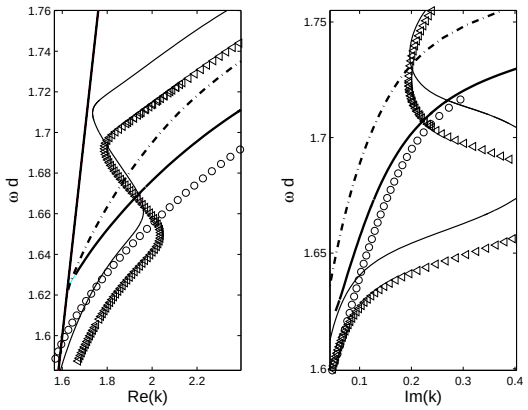

Fig. 5. Real and imaginary part of $k(\omega)$ for the mode $T_{2a}L_i$ and L_iT_{2a} (theoretical results: black thin line; FEM results: triangles) and L_aT_{2i} (theoretical results: black bold line; FEM results: circles). The black dashdot line is relative to mode L in the single chain. The curve relative to $T_{2a}L_i$ flows into that of L_iT_{2a} starting from $\omega d \approx 1.72$

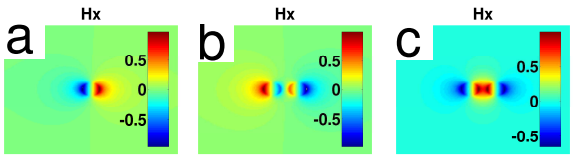

Fig. 6. Field H_x of modes T_1 in the single chain (a, $\omega d = 1.50$) and of modes T_{1i} (b, $\omega d = 1.50$) and T_{1a} in the double chain (c, $\omega d = 1.59$)

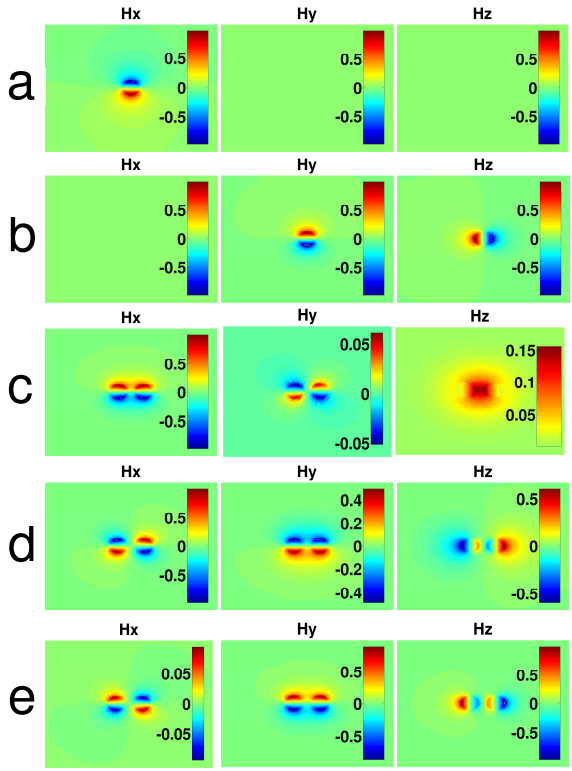

Fig. 7. Fields H_x, H_y and H_z of modes T_2 (a, $\omega d = 1.50$) and L (b, $\omega d = 1.70$) in the single chain and of modes $T_{2i}L_a$ (c, $\omega d = 1.34$), $T_{2a}L_i$ (d, $\omega d = 1.70$) and L_iT_{2a} (e, $\omega d = 1.76$) in the double chain

References

1. E. Ozbay, *Plasmonics: Merging photonics and electronics at nanoscale dimensions*, Science **311,** 189-193 (2006).

2. S. A. Maier, *Plasmonics: Fundementals and Applications*, Springer (2007)

3. E. N. Economou, *Surface plasmons in thin films*, Phys. Rev. **182**, 539 (1969).

4. G. Veronis and S. Fan, *Bends and splitters in metal-dielectric-metal subwavelength plasmonic waveguides*, Appl. Phys. Lett. **87**, 131102 (2005).

5. E. Moreno, S. G. Rodrigo, S. I. Bozhevolnyi, L. Martin-Moreno, and F. J. Garcia-Vidal, *Guiding and Focusing of Electromagnetic Fields withWedge Plasmon Polaritons*, Phys. Rev. Lett. **100**, 023901 (2008).

6. E. Moreno, F. J. Garcia-Vidal, S. G. Rodrigo, L. Martin-Moreno, and S. I. Bozhevolnyi, *Channel plasmon-polaritons: modal shape, dispersion, and losses*, Opt. Lett. **31**, 3447 (2006).

7. M. Quinten, A. Leitner, J.R. Krenn, and F. R. Aussenegg, *Electromagnetic energy transport via linear chains of silver nanoparticles*, Opt. Lett. **23,** 1331-1333 (1998).

8. M. L. Brongesma, J. W. Hartman, and H. A. Atwater, *Electromagnetic energy transfer and switching in nanoparticle chain arrays below the diffraction limit*, Phys. Rev. B **62,** R16356-R16359 (2000).

9. S. A. Maier, P. G. Kik, and Harry A. Atwater, *Optical pulse propagation in metal*

nanoparticle chain waveguides, Phys. Rev. B **67,** 205402 (2003).

10. W. H. Weber and G. W. Ford, *Propagation of optical excitations by dipolar interactions in metal nanoparticle chains*, Phys. Rev. B **70,** 125429 (2004).

11. D. S. Citrin, *Coherent excitation transport in metal-nanoparticle chains*, Nano Lett. **4,** 1561-1565 (2004).

12. R. A. Shore and A.D. Yaghjian, *Travelling electromagnetic waves on linear periodic arrays of lossless spheres*, Electron. Lett. **41,** 578-580 (2005).

13. C. R. Simovsky, A. J. Viitanen, and S. A. Tretyakov, *Resonator mode in chains of silver nanoparticles and its possible application*, Phys. Rev. E **72,** 066606 (2005).

14. D. S. Citrin, *Plasmon-polariton transport in metal-nanoparticle chains embedded in a gain medium*, Opt. Lett. **31,** 98-100 (2006).

15. A. F. Koenderink and A. Polman, *Complex response and polariton-like dispersion splitting in periodic metal nanoparticle chains*, Phys. Rev. B **74,** 033402 (2006).

16. A. Alú and N. Engheta, *Theory of linear chains of metamaterial/plasmonic nanoparticles as a subdiffraction optical nanotrasmission lines*, Phys. Rev. B **74,** 205436 (2006).

17. V. A. Markel and A.K. Sarychev, *Propagation of surface plasmons in ordered and disordered chains of nanoparticles*, Phys. Rev. B **75**, 085426 (2007).

18. A. A. Govyadinov and V. A. Markel, *From slow to superluminal propagation: Dispersive properties of surface plasmon polaritons in linear chains of metallic*

nanospheroids, Phys. Rev. B **78**, 035403 (2008).

19. M. Conforti and M.Guasoni , *Dispersive properties of linear chains of lossy metal nanoparticles*, J. Opt. Soc. Am. B **27**, 1576 (2010).

20. H. Chu, W. Ewe1 E. L and R. Vahldieck, *Analysis of sub-wavelength light propagation through long double-chain nanowires with funnel feeding*, Opt. Express **15**, 4217 (2007).

21. A. Alú, P. A. Belov, N. Engehta, *Parallel-chain optical transmission line for a low-loss ultraconfined light beam*, Phys. Rev. B **80**, 113101 (2009).

22. J. M. Gerardy and M. Ausloos, *Absorption spectrum of spheres from the general solution of Maxwell's equations. II. Optical properties of aggregated metal spheres*, Phys. Rev. B **25**, 4204 (1982).

23. Y-l. Xu , *Fast evaluation of the Gaunt coefficients*, Math. Comput. **65**, 1601 (1996).

24. A. Erdelyi, W. Magnus, F. Oberhettinger, F. G. and Tricomi, *Higher Transcendental Functions, Vol. 1*, New York: Krieger, (1981).

25. P. B. Johnson and R. W. Christy, *Optical constants of noble metals*, Phys. Rev. B, vol. 6, 4370-4379 (1972).

26. J.D.Joannopoulos, R.D. Meade and J.N.Winn *Photonic Crystals: molding the flow of light* (2008).